Contract No:

This document was prepared in conjunction with work accomplished under Contract No. DE-AC09-08SR22470 with the U.S. Department of Energy (DOE) Office of Environmental Management (EM).

Disclaimer:

United States Department of Energy

Savannah River Site

Electromagnetic Borehole Flowmeter Testing at the H-Area Extraction Wells (U)

WSRC–TR–2002-00187
Revision 0
May 2002

Prepared by:
Westinghouse Savannah River Company LLC
Savannah River Site
Aiken, SC 29808
Prepared for the U. S. Department of Energy Under Contract No. DE-AC09-96SR18500

DISCLAIMER

Printed in the United States of America

Prepared for
U.S. Department of Energy
and
Westinghouse Savannah River Company LLC
Aiken, South Carolina

Approvals:

Gregory P. Flach, Author Date

Mary K. Harris, L4 Manager Date

P. Casey Knapp, ERD -Project Task Team Lead Date

TABLE OF CONTENTS

LIST OF FIGURES

LIST OF TABLES

LIST OF ACRONYMS AND ABBREVIATIONS

cm	centimeter
CPT	cone penetrometer testing
EBF	electromagnetic borehole flowmeter
GEL	General Engineering Laboratory
L/min	liter per minute
mL	milliliter
msl	mean sea level
pCi	picocurie
TOC	top of casing

1.0 INTRODUCTION

Electromagnetic Borehole Flowmeter (EBF) testing has been used at several locations at the Savannah River Site to characterize hydraulic conductivity variation along well screens (Phifer 1996, Boman et al. 1997, Flach et al. 2000a and b, Flach et al. 2001). The objective of the EBF testing documented in this report is to expand the technology to include simultaneous characterization of conductivity, contaminant concentration, and mass flux profiles. The latter two parameters, especially mass flux, can be valuable information for remedial design.

Mass flux refers to contaminant mass flow rate per unit length of well screen. The basic idea is to take samples of the groundwater passing through the EBF and have them analyzed in the laboratory for contaminant concentration. The product of EBF flow and laboratory concentration provides an estimate of the mass flux entering the portion of the well screen below the EBF. The cumulative flow and mass flux data can then be used to find conductivity, concentration and mass flux entering the well along each screen interval. This expanded capability has been demonstrated for tritium at three extraction wells associated with the H-area seepage basin pump and treat-reinject remediation system, HEX-3, HEX-4 and HEX-18. Figure 1 shows the locations of these wells and Table 1 provides basic well construction information.

This study was initiated through Technical Assistance Request ERE-TAR-2001-0027 and conducted in accordance with a Task Technical and Quality Assurance Plan (Flach and Ekechukwu 2001).

1.1 Test Design

The use of an EBF to determine the vertical variation in horizontal hydraulic conductivity along a well screen has been documented (e.g., Waldrop 1995; Molz and Young 1993; Flach et al. 2000a). Past Savannah River Site applications include Phifer (1996), Boman et al. (1997), and Flach et al. (2000a, b). The EBF measures *vertical* flow inside a well casing based on Faraday's Law of Induction, which states that the voltage induced by a conductor moving at right angles through a magnetic field is directly proportional to the velocity of the moving conductor (Waldrop 1995). Schematic diagrams of the EBF are shown in Figures 2 and 3 (Molz and Young 1993). In this application, groundwater acts as the moving conductor, an electromagnet generates the magnetic field, and the electrodes measure the induced voltage.

The idea behind EBF testing is to relate horizontal conductivity as a function of elevation, K(z), to borehole discharge as a function of elevation Q(z). The field procedure is schematically illustrated in Figure 4. Under quasi-steady pumping conditions, borehole discharge (Q) from the bottom of the screen up to the current flowmeter position is measured as a function of elevation (z). As shown in Figure 5, the difference (ΔQ) in borehole discharge Q(z) between any two locations is the flow rate of groundwater entering the well casing over that interval. This differential flow rate, minus any ambient flow effects, is directly proportional to the horizontal conductivity of the aquifer over that interval. The data analysis procedure is summarized by

$$\frac{K_i}{\overline{K}} = \frac{(\Delta Q_i - \Delta q_i)/\Delta z_i}{\sum_i (\Delta Q_i - \Delta q_i) \Big/ \sum_i \Delta z_i} \tag{1}$$

where:

K_i ≡ horizontal conductivity of the i^{th} interval

$\overline{K}$ ≡ vertically-averaged conductivity

ΔQ_i ≡ difference in EBF flow at the top and bottom of the i^{th} interval under *pumping* conditions

Δq_i ≡ difference in EBF flow at the top and bottom of the i^{th} interval under *ambient* conditions

Δz_i ≡ height of the i^{th} interval.

In equation (1), $(\Delta Q_i - \Delta q_i)$ is the net flow rate induced by pumping and accounts for ambient flow effects. Ambient flow refers to horizontal flow through the well screen and vertical flow in the casing under natural, undisturbed conditions. Note that the relative conductivity distribution is equal to the relative distribution of net flow entering the well, which is assumed to occur after the initial transient passes and after quasi-steady state conditions develop.

To determine concentration and mass flux distributions, additional measurements are needed. By measuring the concentration of a contaminant in groundwater passing through the EBF at each elevation, the mass flux entering the wellbore over the i^{th} interval can be computed from

$$m_i = Q_{i+1}C_{i+1} - Q_iC_i \qquad (2)$$

where

m_i = mass flux entering the wellbore over the i^{th} interval

Q_i = cumulative flow entering the wellbore from the bottom of the screen up to the i^{th} elevation

C_i = concentration in the cumulative flow passing through the EBF at the i^{th} elevation

The concentration in the formation at the i^{th} screen interval is computed from

$$c_i = \frac{m_i}{\Delta Q_i} = \frac{Q_{i+1}C_{i+1} - Q_i C_i}{Q_{i+1} - Q_i} \tag{3}$$

where

c_i = concentration in groundwater entering the wellbore over the i^{th} interval.

Equations (1) through (3) summarize the technical basis for the borehole flowmeter testing in groundwater monitoring wells planned for the HEX wells.

1.2 Test Equipment

A schematic diagram showing the configuration of the primary equipment used to perform the field test is shown in Figure 6. Borehole flow measurements were taken using a Century Geophysical Corporation system consisting of the downhole EBF instrument, a 300-meter drawworks, and a Compu-Log data acquisition computer. Well discharge was induced using a Grundfos Redi-Flo2 submersible pump mounted on a center discharge hose reel and driven by a variable speed controller. Groundwater samples were taken using a small bladder pump operated through an electronic controller supplied with compressed nitrogen, and attached to 85 ft of 1/4" tubing on a reel. Both of the pumps were mounted on the EBF instrument and traveled together as a unit by operating the drawworks. A portable generator and uninterruptable power supply provided electrical power.

1.3 Test Procedures

To rigorously account for potential ambient flow effects, the standard borehole flowmeter test procedure entails two series of measurements acquired through the following actions:

1) Under ambient conditions, measure the vertical flow rate inside the well screen at 1- to 2-ft intervals.

2) Pump (or inject) at a constant rate above the screen zone and borehole flowmeter.

3) Pause until the drawdown reaches a quasi-steady-state.

4) Under these quasi-steady-state pumping conditions, again measure the vertical flow rate inside the well screen at 1- to 2-ft intervals.

If ambient flows are small compared to dynamic flows, step 1 may be omitted. The quasi-steady-state conditions referred to in step 3 typically occur within 15 to 30 minutes in confined aquifers and within a couple of hours in unconfined aquifers.

For testing at the HEX wells, a 2-ft measurement interval was chosen. Ambient flows were expected to be small so ambient flowing testing was assumed to be unnecessary. The ambient test was performed at HEX-4 to check this assumption. Under dynamic (pumping) conditions, a 100-mL groundwater sample was acquired with each flow measurement. The GEL Mobile Laboratory performed tritium analyses on the groundwater samples. Instrument calibration and field procedures were documented by Flach and Ekechukwu (2001a) and in Controlled Notebook WSRC-NB-2001-00167.

1.4 HEX-3 Data Analysis

EBF testing was performed on HEX-3 on February 4, 2002, between approximately 11:30 AM and 3:30 PM. The extraction system pump was shut off approximately 24 hours in advance of EBF testing. Preliminary field and laboratory data are presented in Table 2. The rubber skirt used to create a seal between the borehole flowmeter tube and well casing allowed personnel to locate the beginning and end of wire-wrap screen sections by feel. Specifically, the EBF assembly would often "hang up" at the start of each screen section as the rubber gasket encountered the longitudinal spacer ribs (Figure 7). Slack or tightening in the drawworks cable was observed in these cases. By monitoring cable tension, personnel determined that the 15-ft screen interval comprised a 5-ft section on top of a 10-ft section (Table 2). The top of the screen appeared to be approximately 1 ft deeper than indicated on the well construction diagram.

The rubber skirt provides a good seal along a smooth well casing, but only a partial seal along the wire-wrap screen because of the longitudinal spacer ribs (Figure 7). Consequently, the EBF generally measures a fraction of the flow that enters the screen and moves up the wellbore. However, at the joint between two screen sections where the inner wall is smooth, the rubber gasket apparently forces all flow through the EBF. This is indicated by the raw flow rate data from HEX-3 (shown in chronological order) in Figure 8. Flow measurements were taken at 2-ft intervals marching up the screen, and then back down the screen. Depth measurements were referenced to the top of the protective casing. After the measurement at a 28.5 ft depth during the downward series of measurements, the EBF was moved back to 27.5 ft where the joint between screen sections occurs. Here the flow reading was substantially higher than those of the surrounding two measurements. The high flow reading was confirmed after the downward run was completed, when the EBF was repositioned to 27.5 ft to conclude testing. At the joint, the EBF-measured flow is roughly twice that immediately above and below.

The precise fraction of total flow passing through the EBF is estimated to be 0.53 in Table 2.

At depths where two readings were taken, the best-estimate is taken as the average of the two measurements. The total flow entering the wellbore below a measurement interval can be estimated by dividing the best-estimate EBF reading by the bypass flow ratio, 0.53, except at the joint between screen sections. Figure 9 shows the result of averaging and correcting for bypass flow. It also shows the flow rate of the Redi-Flo2 pump, corrected for head losses between the diversion valve where bucket-and-stopwatch measurements were taken and the radiological "buffalo" tank. The correction is based on post-test experimentation at 704-D that indicated the additional tubing past the diversion valve results in a 10% flow reduction (WSRC-NB-2001-00167). The Redi-Flo2 pumping rate corresponds to the total flow entering the wellbore.

The flow profile shown in Figure 9 is peculiar in that the cumulative flow rate decreases between an elevation of 9 and 11 ft (depths of 28.5 and 26.5 ft). In principle, the cumulative flow log should be strictly non-decreasing. That is, flow should increase or, at worst, equal that of the next lower station (Figure 4). Technically this statement is only true of the net difference between dynamic and ambient flow rates (cf. eqn. (1)). Ambient testing was not performed at HEX-3; however, as expected, the ambient flows measured in nearby HEX-4 were negligible compared to the dynamic flows. Therefore, ambient flow does not explain the cumulative flow decreases. Instrument error is another possible reason for these decreases but this is unlikely because the basic shape reflected on the graph was reproduced as the instrument moved up and down the borehole. Moreover, no significant drift was observed in the instrument under zero flow conditions at either the start or the end of the field test. Second-order effects such as "head-loss-induced flow redistribution" (Dinwiddie et al. 1999; Flach et al.

2000a) and hydraulic diffusivity contrasts between formation layers (Kabala 1994, Ruud and Kabala 1996, Flach et al. 2000a) can impact the EBF flow log but not to the extent observed in Figure 9.

The most likely explanation for the unexpected behavior in Figure 9 is significant variation in the fraction of the flow passing through the EBF versus bypassing the instrument, both between the skirt and well casing, and outside the screen in the filter pack annulus (Figure 7). A likely cause is that the filter pack annulus along the upper portion of the HEX-3 screen is much more conductive than at lower elevations. Changes in filter pack conductivity are thought to have caused a similar sudden reduction in flow during EBF testing at RPC-3PW (Flach et al. 2000a). Another possibility is fouling and scale buildup inside the well screen, both of which might affect the seal between the EBF rubber gasket and well screen.

Whatever the root cause, a reduction in cumulative EBF flow leads to a non-physical, negative value for hydraulic conductivity for the interval between a depth of 26.4 and 28.4 ft, as shown in the remainder of Table 2. A negative flow rate, combined with the GEL mobile lab tritium data from Appendix A, also produces a non-physical negative value for interval mass flow rate. The results of this preliminary analysis are plotted in Figure 10. Knowing that the flow log should be non-decreasing, better estimates are achieved by interpreting what the flow rates might have been under more ideal test conditions. Under ideal conditions bypass flow is a constant fraction of total flow and the measured EBF flow is non-decreasing. One such possibility of the actual variation in borehole flow is shown in Figure 9. The corresponding hydraulic conductivity, tritium concentration, and mass flux profiles are shown in Figure 11 and Table 3. Given uncertainty in the interpretation, the revised profiles in Figure 11 should be used in a semi-quantitative manner.

The data in Figure 11 indicate that groundwater enters the lower half of the screen at roughly three times the rate that it enters along the upper half of the screen. The variability in tritium concentration is low compared to the permeability variation. As a result, the mass flux profile follows the same trend as permeability. The shape of the concentration profile determined from EBF testing appears to be consistent with cone penetrometer testing (CPTs) conducted approximately 85 ft upgradient of HEX-3 (Appendix B). However, the average CPT sample concentration is approximately 2,700 pCi/mL compared to 654 pCi/mL for the screen average during EBF testing, a factor of 4 difference. The concentration of groundwater samples taken from HEX-3 on September 20, 2001, was 505 pCi/mL, which is similar to the EBF results. The reason for the discrepancy between the HEX-3 sampling results and CPT is uncertain, but two plausible explanations can be offered. First, the friction ratio log for HCPT-03 indicates the CPT groundwater samples with tritium concentrations exceeding 3,000 pCi/mL came from finer-grained sediments, i.e., silts and clays (Appendix B). Such sediments have lower permeability and do not contribute much groundwater to a sample obtained after well purging or pumping has been performed. In other words, the concentration from HEX-3 is a flow-weighted average of concentrations in the formation outside the screen. A second explanation is that, despite being reasonably close (85 ft), the CPT push and HEX-3 lie on different flow paths with different tritium concentrations.

1.5 HEX-4 Data Analysis

EBF testing was performed on HEX-4 on February 6, 2002, between approximately 10:00 AM and 2:00 PM. The extraction system pump was shut off approximately 24 hours in advance of EBF testing. An analysis of EBF field data and laboratory sample results for HEX-4 is presented in Table 4. An initial EBF test of ambient flow conditions indicated a slight upward flow, probably corresponding to ongoing well recovery following pump shutdown the day before.

The ambient flow rates were very small compared to dynamic testing rates. A single measurement was taken at each measurement interval. The cumulative flow profile for HEX-4 shown in Figure 12 shows none of the peculiarities observed in HEX-3. Specifically, the profile exhibits no significant decreases in low rate as the EBF advances upward. However, these observations do not preclude varying bypass flow or other problems similar to those observed with HEX-3. Relative conductivity, tritium concentration, and mass flux profiles are shown in Figure 13. Here the flow and hydraulic conductivity data show the opposite trend as HEX-3. Almost no flow enters the lower 40% of HEX-4. Like HEX-3, the tritium concentration exhibits less vertical variation than permeability, and the mass flux profile is again similar to the conductivity profile. According to EBF testing, the tritium concentration tends to increase going from the screen top to bottom. This is qualitatively consistent with the nearby CPT results listed in Appendix B. However, the well average concentration of 365 pCi/mL was again much lower during EBF testing compared to the average CPT result (Appendix B). Groundwater samples taken from HEX-4 on September 20, 2001, averaged 494 pCi/mL, which is closer to the EBF sampling results. The reason for the discrepancy between the HEX-4 sampling results and CPT is uncertain. The two potential explanations offered above for HEX-3 hold for HEX-4 as well.

1.6 HEX-18 Data Analysis

EBF testing was performed on HEX-4 on February 11, 2002, between approximately 1:00 PM and 5:00 PM. The pump in HEX-18 was shut off approximately 8 hours in advance. Table 5 presents field and laboratory data for HEX-18. Figure 14 shows the cumulative flow log corrected for bypass flow. Like HEX-4, the cumulative flow data show an unexpected decrease in flow rate in the upper portion of the screen. Unfortunately, multiple measurements at each station were not possible due to time limitations in the field, and an instrument problem could not be ruled out. This possibility is still considered unlikely as the

EBF showed no zero drift. Variable bypass flow is considered the most likely explanation. Conductivity, concentration, and mass flux profiles using unaltered data are presented in Figure 15. To avoid non-physical behavior in the end results, the flow data are reinterpreted in a manner similar to HEX-3 (Table 6 and Figure 14). Specifically, the cumulative flow curve was revised so that it would increase continuously along the upper portion of the screen, as shown by the dashed line. The revised estimates are presented in Figure 16.

Again, given uncertainty in the interpretation, these results should be used in a semi-qualitative manner. According to the EBF testing results, approximately 75% of the total flow comes from only a 4-ft interval near the bottom of the screen. The concentration profile shows a trend of decreasing concentration with depth, but the trend is less pronounced than the CPT results shown in Appendix B. The average well concentration during EBF testing was 1,770 pCi/mL compared to roughly 1,300 pCi/mL for CPT. The agreement is good relative to the HEX-3 and -4 comparisons. The friction ratio log for HCPT-01A indicates the CPT groundwater samples of interest came from coarser-grained sediments, i.e., sands and silts. These higher permeability sediments would significantly affect groundwater samples taken after well purging or pumping had been performed.

2.0 DISCUSSION

The new EBF system from Century Geophysical Corporation used in HEX well testing appears to have performed well after earlier warranty repairs (Flach et al. 2001b), but instrument drift during HEX testing cannot be completely ruled out. The concept of simultaneous measurement of hydraulic conductivity, contaminant concentration, and mass flux appears to be sound. However, variable amounts of flow bypassing the borehole flowmeter apparently compromised the quality of test results from HEX wells, which are equipped with a wire-wrap screen and filter pack. Bypass flow by itself is not a serious problem, but rather varying amounts of bypass flow relative to total wellbore flow. The cumulative EBF flow log can be effectively corrected for a uniform fraction of bypass flow, but not for the variable amount apparent in testing at HEX-3 and -18. Therefore, the conductivity, concentration, and mass flux profiles derived at the HEX wells contain more uncertainty than desired and inherent in the technology.

3.0 RECOMMENDATIONS

Flow bypassing the EBF continues to compromise the effectiveness of borehole flowmeter testing. For future EBF testing, the following actions are recommended to the extent feasible to reduce bypass flow or at least to make it more uniform along the well screen:

1) Use a slotted screen rather than wire-wrap screen. The smooth inner wall of a slotted screen allows for a good seal with the EBF rubber gasket.

2) Use minimal or no filter pack. The absence of a high conductivity pathway outside the screen minimizes flow bypassing the EBF outside the well casing.

3) Consider re-developing an old well with a filter pack as a potential method of achieving a more uniform filter pack conductivity and bypass flow.

4) Inspect the inside of the well screen for fouling and scale buildup or other features that could cause variable bypass flow, and clean or swab if needed

5) Improve the design of the EBF skirt to reduce the fraction of flow bypassing the instrument inside the screen. Suggested design improvements include adding additional skirts and resizing the gasket and supporting flange diameters.

6) Because the ideal arrangement is a slotted screen well with no filter pack, consider installing a 2" slotted screen well with CPT, letting the natural formation collapse around the screen.

4.0 REFERENCES

Boman, G. K., F. J. Molz and K. D. Boone, 1997. Borehole Flowmeter Application in Fluvial Sediments: Methodology, Results, and Assessment, Ground Water, v35 n3

Controlled Notebook WSRC-NB-2001-00167

Dinwiddie, C. L., N. A. Foley and F. J. Molz, 1999. In-well Hydraulics of the Electromagnetic Borehole Flowmeter, Ground Water v37 n2, 305-315

Flach, G. P., F. C. Sappington, W. Pernell Johnson and R. A. Hiergesell, 2000a. Electromagnetic Borehole Flowmeter (EBF) Testing in R Area (U), WSRC-TR-2000-00170

Flach, G. P., F. C. Sappington, F. A. Washburn and R. A. Hiergesell, 2000b. Electromagnetic Borehole Flowmeter (EBF) Testing at the Southwest Plume Test Pad (U), WSRC-TR-2000-00347

Flach, G. P., and A. A. Ekechukwu, 2001. Task technical and QA plan for electromagnetic borehole flowmeter testing at the H-area extraction wells (U), WSRC-TR-2001-00426, Rev. 0

Flach, G. P., W. E. Jones and F. C. Sappington, 2001. Borehole flowmeter testing at SWP-100D, Interoffice memorandum SRT-EST-2001-00322

Kabala, Z. J., 1994. Measuring distributions of hydraulic conductivity and specific storage by the double flowmeter test, Water Resources Research, v30 n3, 685-690

Molz, F. J. and S. C. Young, 1993. Development and application of borehole flowmeters for environmental assessment, The Log Analyst, v3, Jan.-Feb., 13-23

Phifer, M. A., 1996. ESS borehole flowmeter capability, Interoffice memorandum SRT-ESS-96-453 dated October 10

Ruud, N. C., and Z. J. Kabala, 1996. Numerical evaluation of flowmeter test interpretation methodologies, Water Resources Research, v32 n4, 845-852

Technical Assistance Request, ERE-TAR-2001-0027

Waldrop, W. R., 1995. A summary of hydrogeologic studies with the Electromagnetic Borehole Flowmeter, report QEC T-102, Quantum Engineering Corporation, 112 Tigitsi Lane, Loudon, Tennessee, 37774, 615-458-0506

5.0 APPENDIX

Appendix A General Engineering Laboratory (GEL) Mobile Lab Tritium Analysis Results

Appendix B Nearby Cone Penetration Test Results

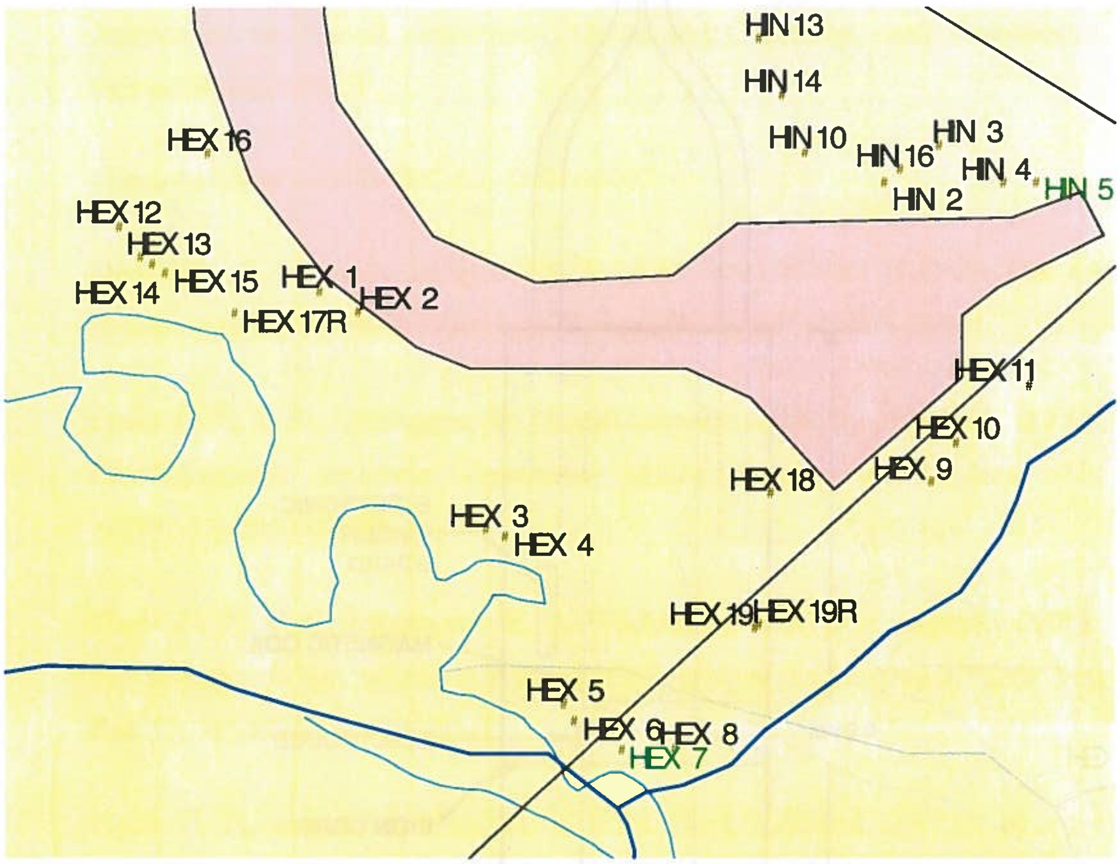

Figure 1. Locations of HEX Wells

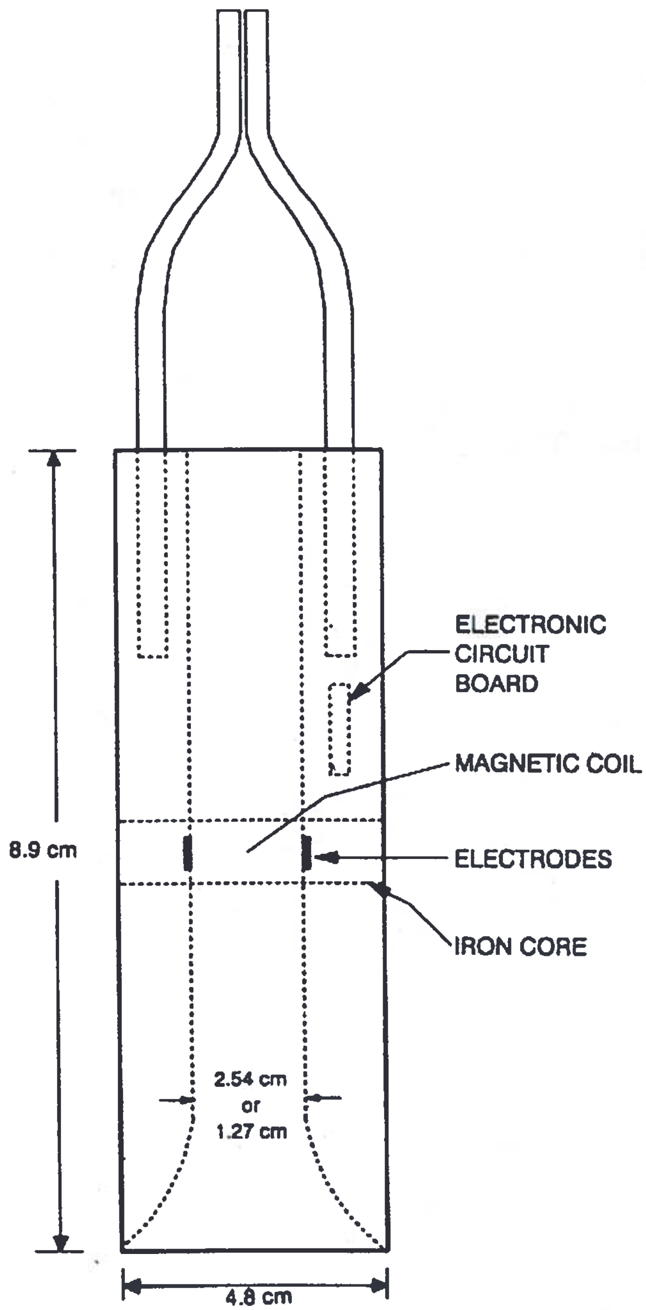

Figure 2. Schematic Diagram of the Electromagnetic Borehole Flowmeter; Reproduced from Molz and Young (1993)

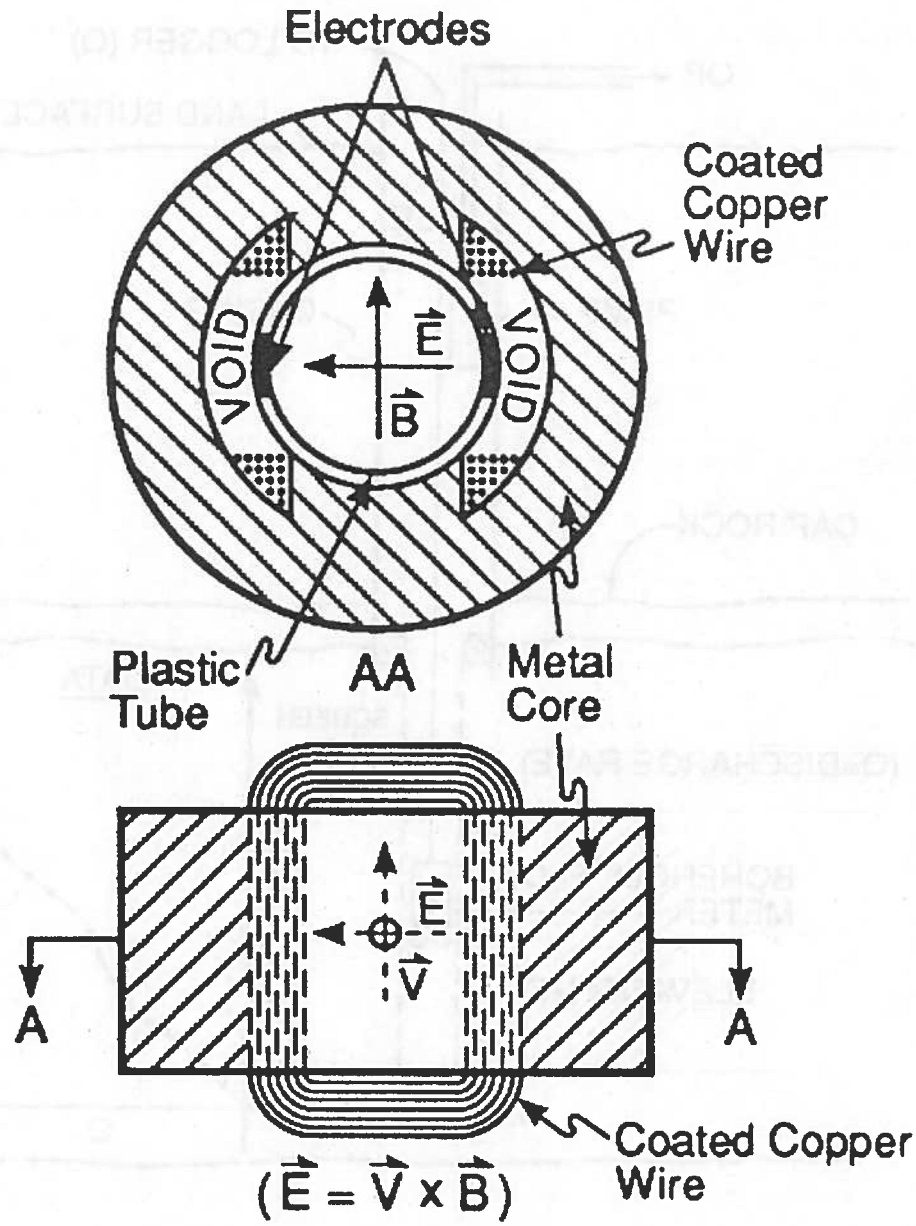

Figure 3. **Electromagnetic Borehole Flowmeter (EBF) Application of Faraday's Law of Induction; Reproduced from Molz and Young (1993)**

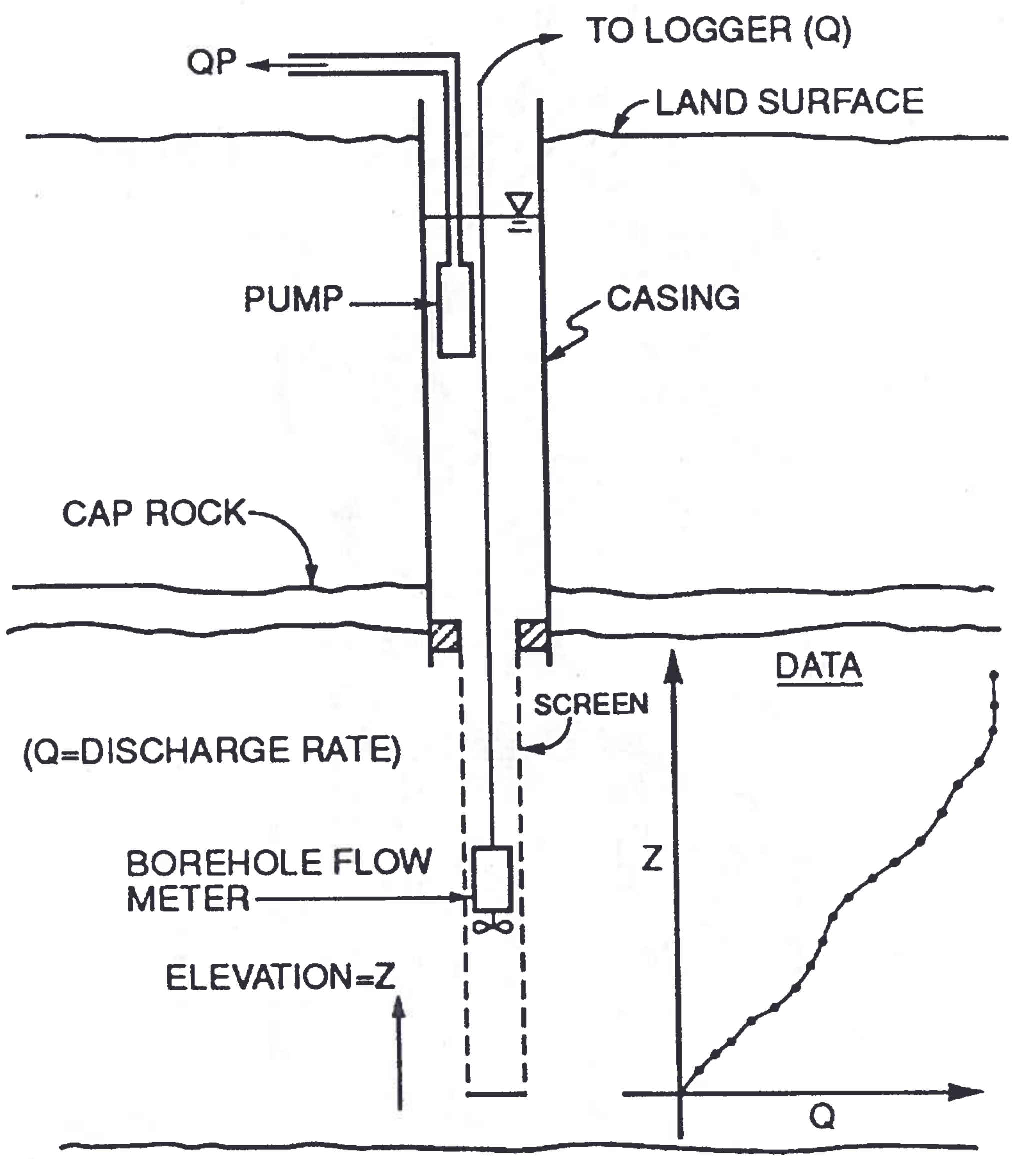

Figure 4. **Schematic Illustration of Borehole Flowmeter Testing; Reproduced from Molz and Young (1993)**

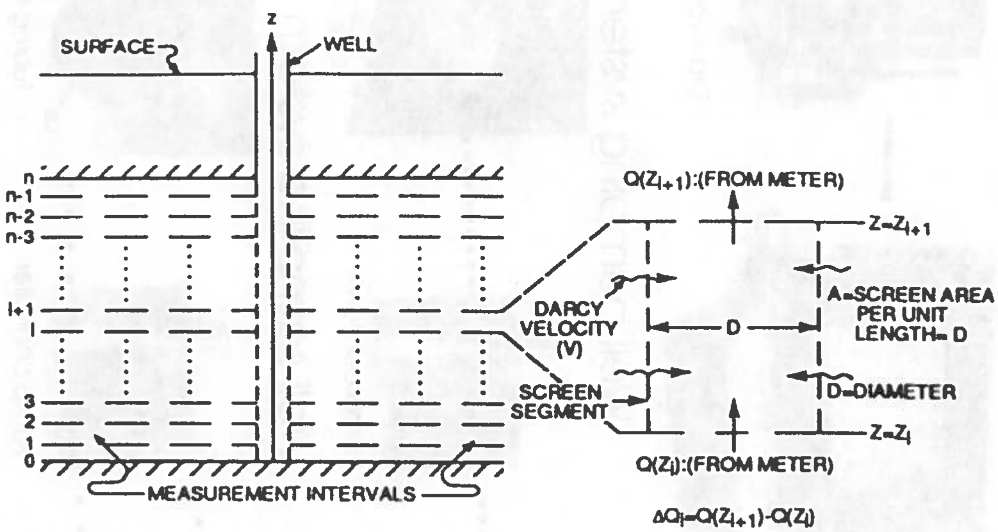

Figure 5. **Basic Geometry and Analysis of Borehole Flowmeter Data; Reproduced from Molz and Young (1993)**

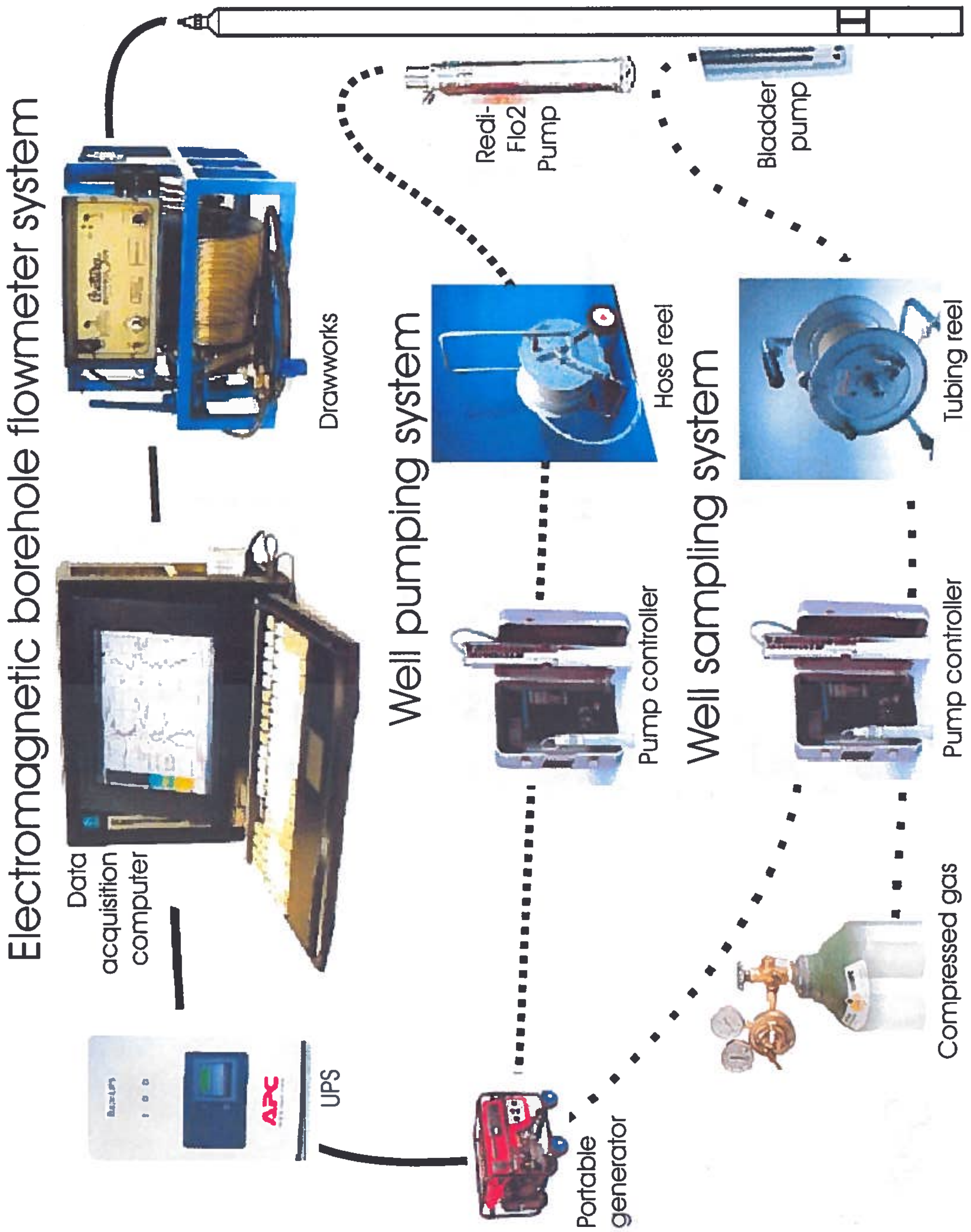

Figure 6. Configuration of Primary Test Equipment

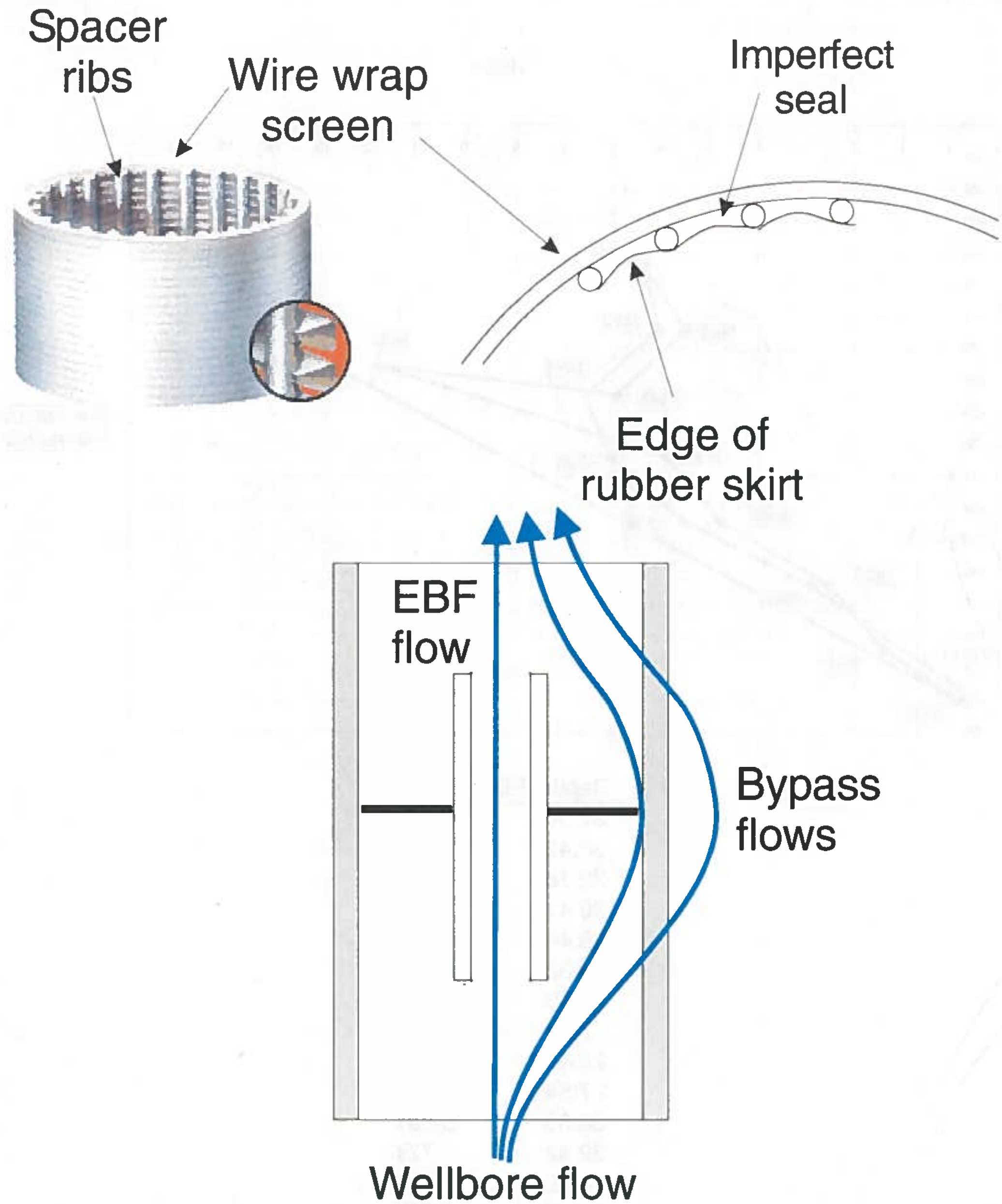

Figure 7. Wire-Wrap Screen Construction and Bypass Flow Phenomenon

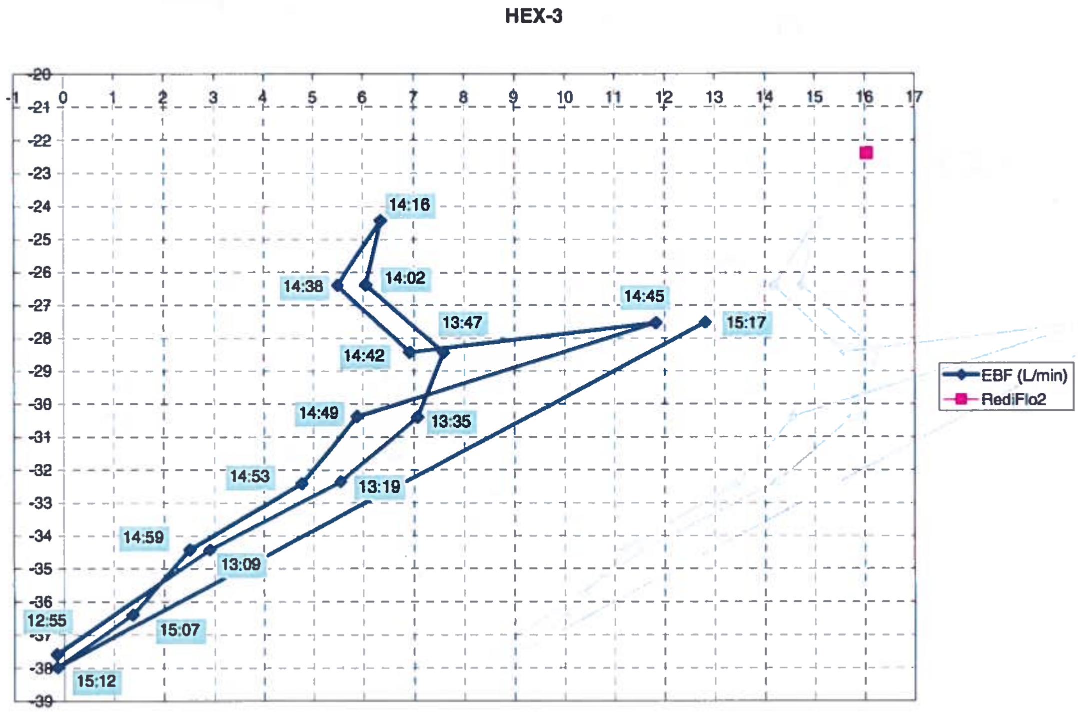

Depth	EBF (L/min)
37.59	-0.149
34.43	2.908
32.36	5.553
30.41	7.067
28.44	7.582
26.38	6.056
24.43	6.346
26.4	5.494
28.43	6.921
27.54	11.831
30.38	5.891
32.42	4.771
34.42	2.508
36.39	1.383
37.99	-0.14
27.53	12.814
22.4	16.047

Figure 8. Raw Flow Data for HEX-3

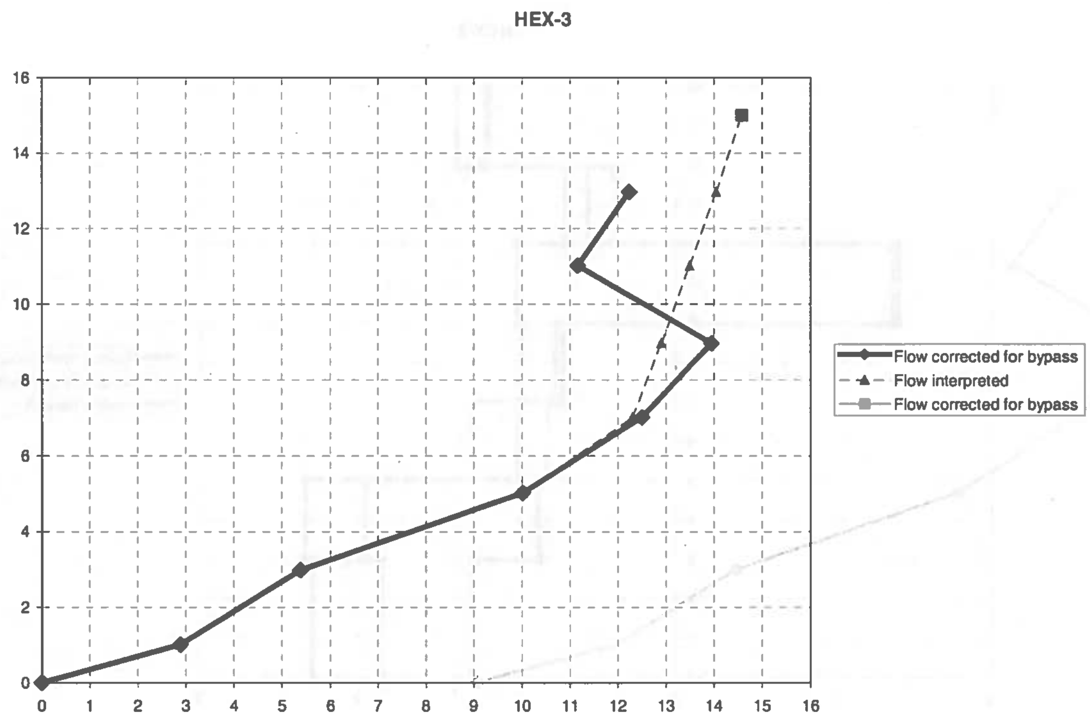

Figure 9. Cumulative Flow Logs for HEX-3, Preliminary and Interpreted

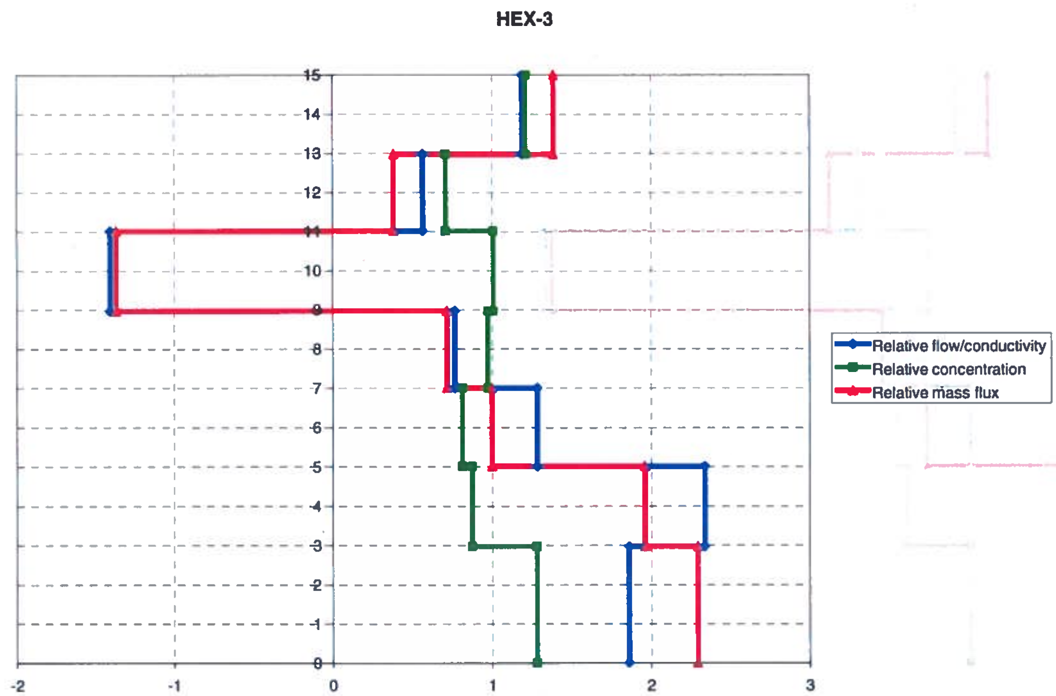

Figure 10. **Preliminary Estimates of Hydraulic Conductivity, Tritium Concentration and Mass Flux, Referenced to Screen Average Values for HEX-3**

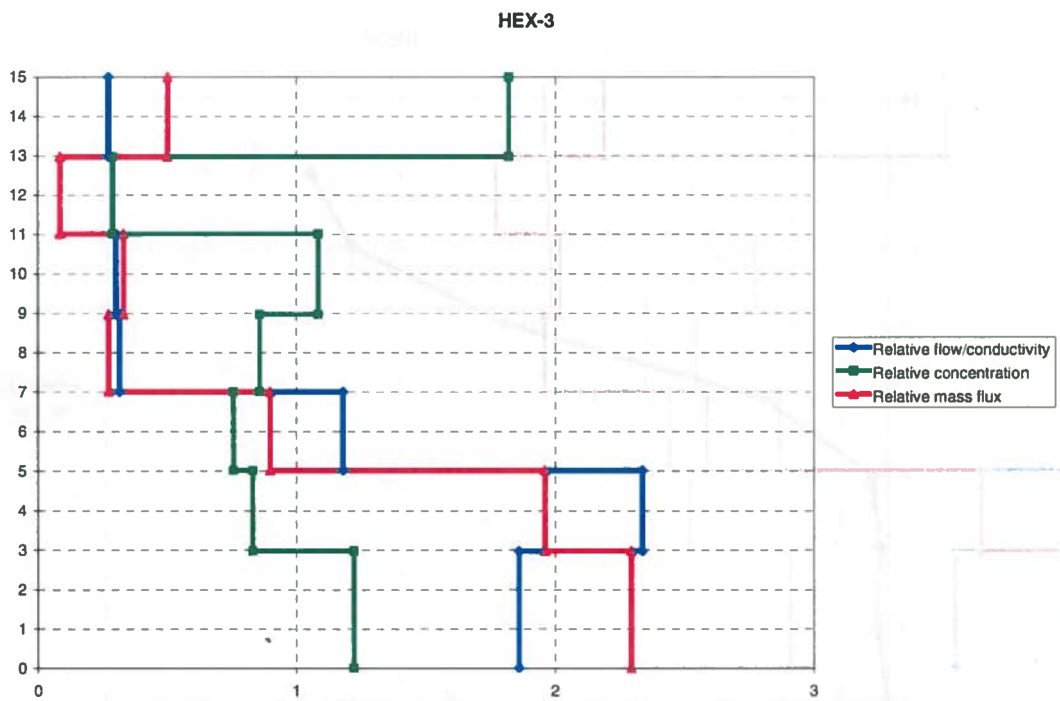

Figure 11. Revised Estimates of Hydraulic Conductivity, Tritium Concentration and Mass Flux, Referenced to Screen Average Values for HEX-3

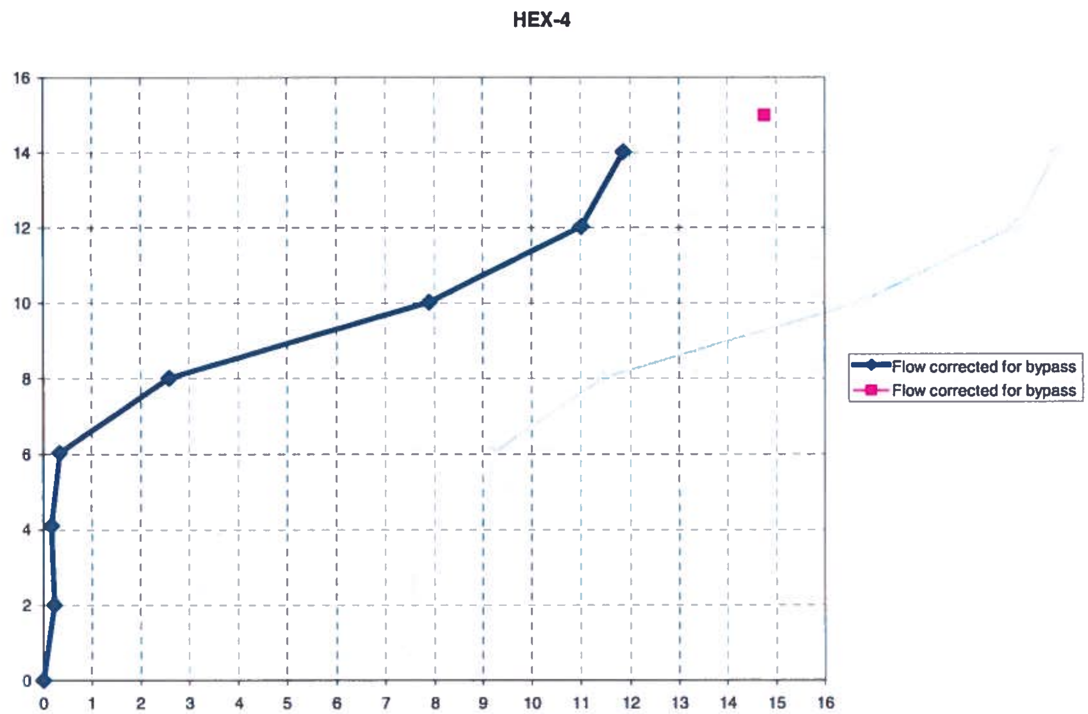

Figure 12. Cumulative Flow Log for HEX-4

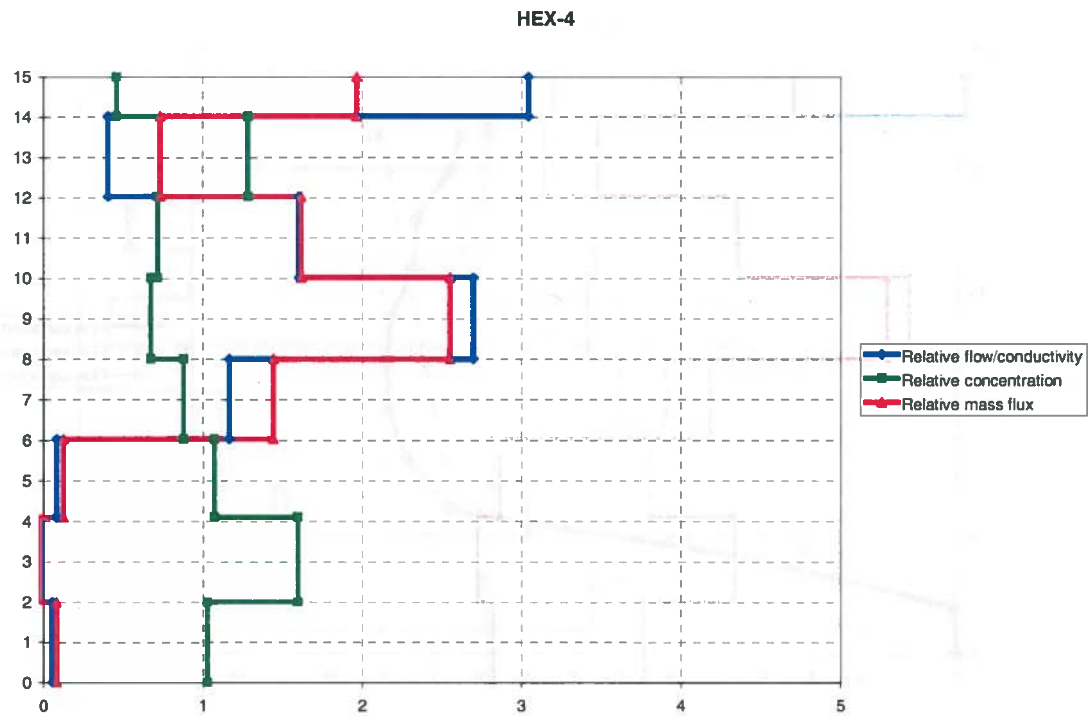

Figure 13. **Estimates of Hydraulic Conductivity, Tritium Concentration and Mass Flux, Referenced to Screen Average Values for HEX-4**

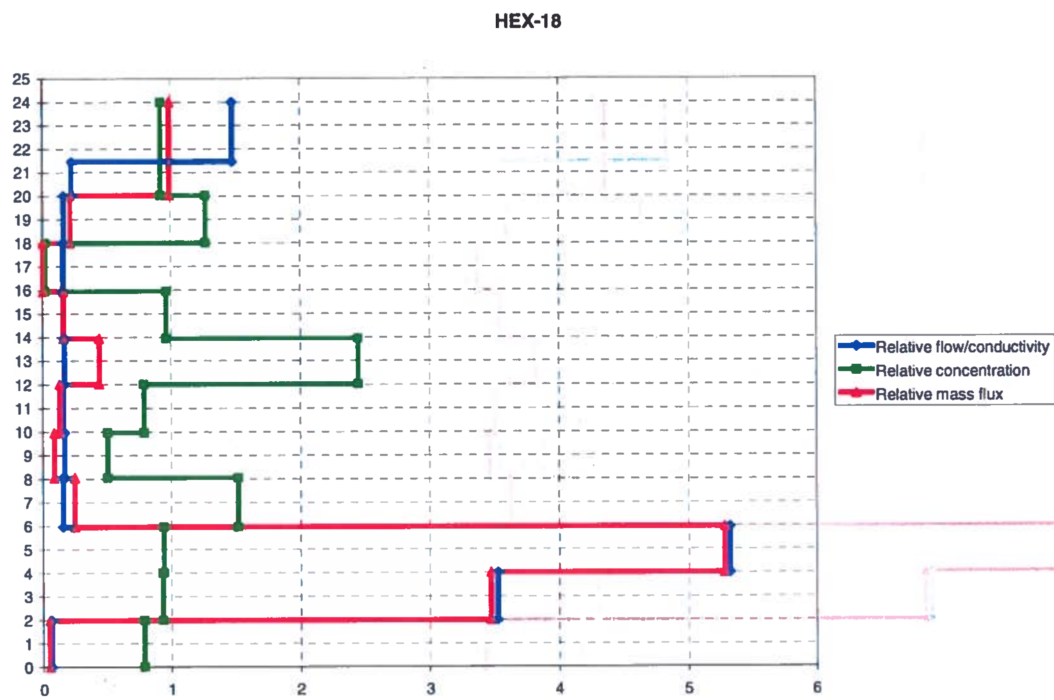

Figure 16. Revised Estimates of Hydraulic Conductivity, Tritium Concentration and Mass Flux, Referenced to Screen Average Values for HEX-18

Well ID	SZ Top (ft MSL)	SZ Bot. (ft MSL)	Grnd. (ft MSL)	TOC (ft MSL)	Eff. Well Depth (ft)	Casing Dia. (in)	Borehole Dia. (in)	Filter Pack Mat'l	SZ Top (ft BGS)	SZ Bot. (ft BGS)	SZ Length (ft)	SZ Top (ft below TOC)	SZ Bot. (ft below TOC)
HEX 1	212.7	192.7	252.7	255.2	62.5	6	14	FX-50	40.0	60.0	20.0	42.5	62.5
HEX 2	219.9	214.9	253.9	254.9	59.9	6	14	SP1-A	34.0	39.0	5.0	35.0	40.0
	205.0	195.0	253.9	254.9					48.9	58.9	10.0	49.9	59.9
HEX 3	209.0	194.1	228.0	229.0	34.9	6	14	SP1-A	19.0	33.9	14.9	20.0	34.9
HEX 4	208.0	193.0	227.0	229.5	36.5	6	14	FX-50	19.0	34.0	15.0	21.5	36.5
HEX 5	195.6	185.6	211.8	215.8	30.2	6	14	FX-50	16.2	26.2	10.0	20.2	30.2
HEX 6	198.1	188.1	211.1	213.1	25.0	6	14	FX-50	13.0	23.0	10.0	15.0	25.0
HEX 7	199.1	189.1	213.1	216.6	27.5	6	14	FX-50	14.0	24.0	10.0	17.5	27.5
HEX 8	199.8	184.9	212.8	215.4	30.5	6	14	FX-50	13.0	27.9	14.9	15.6	30.5
HEX 9	217.6	197.7	240.6	242.6	44.9	6	14	FX-50	23.0	42.9	19.9	25.0	44.9
HEX 10	217.4	202.4	239.4	240.4	38.0	6	14	FX-50	22.0	37.0	15.0	23.0	38.0
HEX 11	218.7	198.8	236.7	238.6	39.9	6	14	SP1-A	18.0	37.9	19.9	20.0	39.9
HEX 12	169.9	164.9	231.9	232.9	113.0	6	14	FX-50	62.0	67.0	5.0	63.0	68.0
	159.9	119.9	231.9	232.9					72.0	112.0	40.0	73.0	113.0
HEX 13	183.0	178.0	232.0	233.0	109.9	6	14	FX-50	49.0	54.0	5.0	50.0	55.0
	173.0	123.1	232.0	233.0					59.0	108.9	49.9	60.0	109.9
HEX 14	178.4	173.4	232.4	233.4	109.9	6	14	FX-50	54.0	59.0	5.0	55.0	60.0
	168.4	123.4	232.4	233.4					64.0	108.9	44.9	65.0	109.9
HEX 15	177.3	167.3	232.4	234.7	112.4	6	14	FX-50	55.2	65.1	10.0	57.5	67.4
	162.3	122.4	232.4	234.7					70.2	110.1	39.9	72.5	112.4
HEX 16	226.5	196.5	258.1	259.1	62.6	6	12.875	SP1-A	31.6	61.6	30.0	32.6	62.6
HEX 17R	209.3	189.4	231.9	232.9	43.5	6	12.875	FX-50	22.6	42.5	19.9	23.6	43.5
HEX 18	218.6	193.7	244.2	245.2	51.5	6	12.875	SP1-A	25.6	50.5	24.9	26.6	51.5
HEX 19R	213.9	199.0	230.9	231.9	32.9	6	12.25	FX-50	17.0	31.9	14.9	18.0	32.9
							FX-50: 0.45 to 0.55 mm						
							SP1-A: 0.84 to 1.68 mm						

*TOC top of casing
*msl mean sea level
*mm millimeter

Table 1. Well Construction Information for HEX Wells

HEX-3

Approximate depths based on EBF rubber skirt resistance - measured from top of protective casing

22.4	screen top
27.4	joint between screen sections
37.4	screen bottom - presumed

EBF "zero" readings (L/min)

-0.149	start of dynamic test (12:55)
-0.140	end of dynamic test (3:12)
-0.145	average

bypass flow estimate

	above	below	joint
	6.056	7.582	11.831
	5.494	6.921	12.814
	average+offset		average+offset
	6.66		12.47
ratio		0.53	

(not used - no ambient test)

	Time	Station ID	Depth below protective casing (ft)	Distance up screen (ft)	EBF reading (L/min)	Zero drift correction (L/min)	Flow corrected for drift (L/min)	Bypass flow factor (unitless)	Flow corrected for bypass (L/min)	Flow corrected for ambient (L/min)	Interval midpoint (ft)	Interval volumetric flow (L/min)	Sample concentration (pCi/mL)	Mass flow (pCi/mL* L/min)	Interval mass flow (pCi/mL* L/min)	Interval concentration (pCi/mL)	Interval mass flux (pCi/mL* L/min)/ft
0	12:55	sump	37.59	0.00	-0.149	0.149	0.000	0.53	0.000	0.000	1.49	5.386		0	4341	806	1459
1	3:07	+1	36.39	1.01	1.383	0.148	1.531	0.53	2.888	2.888							
2	1:09 & 2:59	+3	34.43	2.98	2.708	0.147	2.855	0.53	5.386	5.386	3.99	4.628	806	4341	2539	549	1247
3	1:19 & 2:53	+5	32.39	5.01	5.162	0.146	5.308	0.53	10.014	10.014	6.01	2.483	687	6880	1268	511	636
4	1:35 & 2:49	+7	30.40	7.01	6.479	0.145	6.624	0.53	12.497	12.497	7.99	1.455	652	8148	893	614	456
5	1:47 & 2:42	+9	28.44	8.97	7.252	0.143	7.395	0.53	13.953	13.953	9.99	-2.788	648	9041	-1773	636	-867
6	2:02 & 2:38	+11	26.39	11.01	5.775	0.142	5.917	0.53	11.165	11.165	11.99	1.075	651	7268	480	446	245
7	2:16	+13	24.43	12.97	6.346	0.141	6.487	0.53	12.240	12.240	13.99	2.348	633	7748	1793	763	883
8		+15	22.40	15.00	16.05	0.140	16.047	1.1 *	14.588	14.588		14.59	654	9541	9541		

* consideration of flow loss between diversion valve and buffalo, and drain back through line

Interval thickness (ft)	Relative flow/conductivity (unitless)	Check	Relative mass flux (unitless)	Check	c*Δz (pCi/ml * ft)	Relative concentration (unitless)	Check	Interval midpoint (ft)
2.98	1.86	5.538	2.29	6.826	2398	1.28	3.802	1.49
2.04	2.34	4.759	1.96	3.991	1116	0.87	1.770	3.99
2.00	1.28	2.553	1.00	1.994	1019	0.81	1.616	6.01
1.96	0.76	1.497	0.72	1.404	1203	0.97	1.907	7.99
2.05	-1.40	-2.867	-1.36	-2.788	1301	1.01	2.062	9.99
1.96	0.56	1.106	0.38	0.754	874	0.71	1.386	11.99
2.03	1.19	2.415	1.39	2.819	1550	1.21	2.457	13.99
15.00					631			
		1.000000		1.000000			1.000000	

*l/min liter per minute

Table 2. Preliminary Data Analysis for HEX-3

HEX-3

Approximate depths based on EBF rubber skirt resistance - measured from top of protective casing

22.4	screen top
27.4	joint between screen sections
37.4	screen bottom - presumed

EBF "zero" readings (L/min)

-0.149	start of dynamic test (12:55)
-0.140	end of dynamic test (3:12)
-0.145	average

bypass flow estimate	above	below	joint
	6.056	7.582	11.831
	5.494	6.921	12.814
	average+offset		average+offset
	6.66		12.47
	ratio	0.53	

	Time	Station ID	Depth below protective casing (ft)	Distance up screen (ft)	EBF reading (L/min)	Zero drift correction (L/min)	Flow corrected for drift (L/min)	Bypass flow factor (unitless)	Flow corrected for bypass (L/min)	Flow interpreted (L/min)	Interval midpoint (ft)	Interval volumetric flow (L/min)	Sample concentration (pCi/mL)	Mass flow (pCi/mL* L/min)	Interval mass flow (pCi/mL* L/min)	Interval concentration (pCi/mL)	Interval mass flux (pCi/mL* L/min)/ft
0	12:55	sump	37.59	0.00	-0.149	0.149	0.000	0.53	0.000	0.000	1.49	5.386		0	4341	806	1459
1	3:07	+1	36.39	1.01	1.383	0.148	1.531	0.53	2.888	2.888							
2	1:09 & 2:59	+3	34.43	2.98	2.708	0.147	2.855	0.53	5.386	5.386	3.99	4.628	806	4341	2539	549	1247
3	1:19 & 2:53	+5	32.39	5.01	5.162	0.146	5.308	0.53	10.014	10.014	6.01	2.286	687	6880	1140	499	571
4	1:35 & 2:49	+7	30.40	7.01	6.479	0.145	6.624	0.53	12.497	12.300	7.99	0.600	652	8020	340	566	173
5	1:47 & 2:42	+9	28.44	8.97	7.252	0.143	7.395	0.53	13.953	12.900	9.99	0.600	648	8359	429	715	210
6	2:02 & 2:38	+11	26.39	11.01	5.775	0.142	5.917	0.53	11.165	13.500	11.99	0.550	651	8789	105	191	54
7	2:16	+13	24.43	12.97	6.346	0.141	6.487	0.53	12.240	14.050	13.99	0.538	633	8894	647	1202	319
8		+15	22.40	15.00	16.05	0.140	16.047	1.1 *	14.588	14.588		14.59	654	9541	9541		

* consideration of flow loss between diversion valve and buffalo, and drain back through line

Interval thickness (ft)	Relative flow/conductivity (unitless)	Check	Relative mass flux (unitless)	Check	c*Δz (pCi/ml * ft)	Relative concentration (unitless)	Check	Interval midpoint (ft)
2.98	1.86	5.538	2.29	6.826	2398	1.22	3.634	1.49
2.04	2.34	4.759	1.96	3.991	1116	0.83	1.692	3.99
2.00	1.18	2.350	0.90	1.792	995	0.76	1.508	6.01
1.96	0.31	0.617	0.27	0.534	1109	0.86	1.681	7.99
2.05	0.30	0.617	0.33	0.675	1463	1.08	2.218	9.99
1.96	0.29	0.566	0.08	0.165	375	0.29	0.568	11.99
2.03	0.27	0.553	0.50	1.017	2441	1.82	3.699	13.99
15.00					660			
		1.000000		1.000000			1.000000	

Table 3. Revised Data Analysis for HEX-3

HEX-4

Approximate depths based on EBF rubber skirt resistance - measured from top of protective casing

22.4	screen top
32	joint between screen sections
37.4	screen bottom - presumed

EBF "zero" readings (L/min)

-0.478	start of ambient test (10:44)
-0.419	between ambient and dynamic test (11:46)
-0.590	end of dynamic test (1:50)
-0.496	average

	Time	Station ID	Depth below protective casing (ft)	Distance up screen (ft)	EBF reading (L/min)	Zero drift correction (L/min)	Flow corrected for drift (L/min)	Bypass flow factor (unitless)	Flow corrected for bypass (L/min)	Interval midpoint (ft)	Interval flow (L/min)
0	10:40	sump	37.90	0	-0.478	0.478	0.000	0.5	0.000	1.02	0.111
1	10:51	+2	35.37	2.03	-0.414	0.470	0.056	0.5	0.111	3.01	-0.043
2	10:54	+4	33.41	3.99	-0.427	0.461	0.034	0.5	0.068	5.01	0.015
3	10:57	+6	31.38	6.02	-0.411	0.453	0.042	0.5	0.083	7.00	0.019
4	11:02	+8	29.42	7.98	-0.393	0.444	0.051	0.5	0.103	9.01	0.037
5	11:04	+10	27.37	10.03	-0.366	0.436	0.070	0.5	0.140	10.99	0.003
6	11:08	+12	25.45	11.95	-0.356	0.427	0.071	0.5	0.143	13.48	0.084 est
7		+15	22.4	15		0.419			0.227 est		
		+14							0.210 est		

	Time	Station ID	Depth below protective casing (ft)	Distance up screen (ft)	EBF reading (L/min)	Zero drift correction (L/min)	Flow corrected for drift (L/min)	Bypass flow factor (unitless)	Flow corrected for bypass (L/min)	Flow corrected for ambient (L/min)	Interval midpoint (ft)	Interval volumetric flow (L/min)	Sample concentration (pCi/mL)	Mass flow (pCi/mL* L/min)	Interval mass flow (pCi/mL* L/min)	Interval concentration (pCi/mL)	Interval mass flux (pCi/mL* L/min)/ft
0	11:46	sump	38.01	0.00	-0.419	0.419	0.000	0.5	0.000	0.000	1.00	0.112		0	59	527	29
1	12:25	+2	35.40	2.00	-0.329	0.440	0.111	0.5	0.223	0.112	3.05	-0.018	527	59	-15	821	-7
2	12:35	+4	33.30	4.10	-0.381	0.462	0.081	0.5	0.162	0.093	5.07	0.158	469	44	87	550	45
3	12:40	+6	31.37	6.03	-0.316	0.483	0.167	0.5	0.334	0.251	7.02	2.236	520	130	1010	452	510
4	12:49	+8	29.39	8.01	0.790	0.505	1.295	0.5	2.589	2.486	9.02	5.262	458.5	1140	1812	344	901
5	1:03	+10	27.38	10.02	3.418	0.526	3.944	0.5	7.888	7.748	11.03	3.126	381	2952	1147	367	571
6	1:16	+12	25.37	12.03	4.961	0.547	5.508	0.5	11.017	10.874	13.03	0.780	377	4099	515	661	259
7	1:36	+14	23.38	14.02	5.363	0.569	5.932	0.5	11.863	11.653	14.51	2.892	396	4615	680	235	694
8		+15	22.4	15	16.25	0.590	16.249	1.1 *	14.772	14.545		14.54	364	5294	5294		

* consideration of flow loss between diversion valve and buffalo

Interval thickness (ft)	Relative flow/conductivity (unitless)	Check	Relative mass flux (unitless)	Check	c*Δz (pCi/ml * ft)	Relative concentration (unitless)	Check	Interval midpoint (ft)
2.00	0.06	0.115	0.08	0.167	1054	1.03	2.051	1.00
2.10	-0.01	-0.019	-0.02	-0.043	1724	1.60	3.354	3.05
1.93	0.08	0.163	0.13	0.246	1062	1.07	2.066	5.07
1.98	1.16	2.306	1.44	2.860	894	0.88	1.740	7.02
2.01	2.70	5.426	2.55	5.134	692	0.67	1.347	9.02
2.01	1.60	3.223	1.62	3.251	738	0.71	1.436	11.03
1.99	0.40	0.804	0.73	1.460	1315	1.29	2.559	13.03
0.98	3.04	2.982	1.96	1.926	230	0.46	0.448	14.51
15.00					514			
		1.000000		1.000000			1.000000	

Table 4. Data Analysis for HEX-4

HEX-18

Approximate depths based on EBF rubber skirt resistance - measured from top of protective casing

28	screen top
33	joint between screen sections
43	joint between screen sections
53	screen bottom - presumed
29	WL in well during dynamic test
	EBF "zero" readings (L/min)
-0.735	start of dynamic test (12:55)
-0.926	end of dynamic test (3:12)
-0.831	average

(not used - no ambient test)

	Time	Station ID	Depth below protective casing (ft)	Distance up screen (ft)	EBF reading (L/min)	Zero drift correction (L/min)	Flow corrected for drift (L/min)	Bypass flow factor (unitless)	Flow corrected for bypass (L/min)	Flow corrected for ambient (L/min)	Interval midpoint (ft)	Interval volumetric flow (L/min)	Sample concentration (pCi/mL)	Mass flow (pCi/mL* L/min)	Interval mass flow (pCi/mL* L/min)	Interval concentration (pCi/mL)	Interval mass flux (pCi/mL* L/min)/ft	bypass flow factor estimates
0	2:27	sump	53.98	0.00	-0.735	0.735	0.000	0.56	0.000	0.000	1.00	0.082		0	121	1480	61	
1	2:52	+2	51.01	1.99	-0.705	0.751	0.046	0.56	0.082	0.082	3.00	4.252	1480	121	7419	1745	3673	
2	3:02	+4	48.99	4.01	1.660	0.767	2.427	0.56	4.334	4.334	4.98	6.237	1740	7541	10959	1757	5649	
3	3:08	+6	47.05	5.95	5.137	0.783	5.920	0.56	10.571	10.571	7.00	0.909	1750	18499	1820	2003	867	
4	3:15	+8	44.95	8.05	5.630	0.799	6.429	0.56	11.480	11.480	9.01	0.389	1770	20319	510	1312	267	
5	3:21	+10	43.04	9.96	11.054	0.815	11.869	1	11.869	11.869	10.99	0.038	1755	20829	7	175	3	0.55
6	3:28	+12	40.99	12.01	5.837	0.831	6.668	0.56	11.906	11.906	12.98	-0.075	1750	20836	815	-10845	422	
7	3:35	+14	39.06	13.94	5.779	0.846	6.625	0.56	11.831	11.831	14.94	-0.488	1830	21651	-1573	3226	-787	
8	3:44	+16	37.06	15.94	5.490	0.862	6.352	0.56	11.343	11.343	16.97	-0.029	1770	20078	-51	1770	-25	
9	3:59	+18	35.00	18.00	5.458	0.878	6.336	0.56	11.315	11.315	19.01	-0.705	1770	20027	-1141	1619	-568	
10	4:22	+20	32.99	20.01	9.716	0.894	10.610	1	10.610	10.610	20.74	-0.239	1780	18886	6476	1741	1623	0.57
11	4:37	+21.5	31.54	21.46	4.898	0.910	5.808	0.56	10.372	10.372	22.73	3.958	no sample					
12	n/a	+25	29.00	24.00	15.76	0.926	15.782	1.1 *	14.329	14.329		14.33	1770	25363	25363			0.56

* consideration of flow loss between diversion valve and buffalo

Interval thickness (ft)	Relative flow/conductivity (unitless)	Check	Relative mass flux (unitless)	Check	c*Δz (pCi/ml * ft)	Relative concentration (unitless)	Check	Interval midpoint (ft)	Interval midpoint (ft)	Depth below ground (ft)	Depth below ground (ft)
1.99	0.07	0.137	0.06	0.115	2945	2.18	4.332	1.00	1.00	49.51	49.51
2.02	3.53	7.121	3.48	7.021	3525	2.57	5.184	3.00	3.00	47.50	47.50
1.94	5.39	10.447	5.35	10.370	3408	2.58	5.013	4.98	4.98	45.52	45.52
2.10	0.72	1.522	0.82	1.722	4206	2.95	6.185	7.00	7.00	43.50	43.50
1.91	0.34	0.651	0.25	0.483	2506	1.93	3.686	9.01	9.01	41.50	41.50
2.05	0.03	0.063	0.00	0.006	358	0.26	0.526	10.99	10.99	39.52	39.52
1.93	-0.07	-0.126	0.40	0.771	-20931	-15.95	-30.783	12.98	12.98	37.53	37.53
2.00	-0.41	-0.817	-0.74	-1.488	6451	4.74	9.488	14.94	14.94	35.56	35.56
2.06	-0.02	-0.048	-0.02	-0.048	3646	2.60	5.363	16.97	16.97	33.53	33.53
2.01	-0.59	-1.180	-0.54	-1.080	3255	2.38	4.787	19.01	19.01	31.50	31.50
1.45	-0.28	-0.400	1.54	6.129	6948	2.56	10.219	20.74	22.01	29.77	28.50
2.54	2.61	6.629						22.73		27.77	
24.00					680						
		1.000000		1.000000			1.000000				

Table 5. Preliminary Data Analysis for HEX-18

HEX-18

Approximate depths based on EBF rubber skirt resistance - measured from top of protective casing

28	screen top
33	joint between screen sections
43	joint between screen sections
53	screen bottom - presumed
29	WL in well during dynamic test
	EBF "zero" readings (L/min)
-0.735	start of dynamic test (12:55)
-0.926	end of dynamic test (3:12)
-0.831	average

	Time	Station	Depth below protective casing	Distance up screen	EBF reading	Zero drift correction	Flow corrected for drift	Bypass flow factor	Flow corrected for bypass	Flow interpreted	Interval midpoint	Interval volumetric flow	Sample concentration - modified	Mass flow	Interval mass flow	Interval concentration	Interval mass flux	bypass flow factor estimates
		ID	(ft)	(ft)	(L/min)	(L/min)	(L/min)	(unitless)	(L/min)	(L/min)	(ft)	(L/min)	(pCi/mL)	(pCi/mL* L/min)	(pCi/mL* L/min)	(pCi/mL)	(pCi/mL* L/min)/ft	
0	2:27	sump	53.98	0.00	-0.735	0.735	0.000	0.56	0.000	0.000	1.00	0.082		0	121	1480	61	
1	2:52	+2	51.01	1.99	-0.705	0.751	0.046	0.56	0.082	0.082	3.00	4.252	1480	121	7419	1745	3673	
2	3:02	+4	48.99	4.01	1.660	0.767	2.427	0.56	4.334	4.334	4.98	6.166	1740	7541	10834	1757	5585	
3	3:08	+6	47.05	5.95	5.137	0.783	5.920	0.56	10.571	10.500	7.00	0.200	1750	18375	564	2820	269	
4	3:15	+8	44.95	8.05	5.630	0.799	6.429	0.56	11.480	10.700	9.01	0.200	1770	18939	191	952	100	
5	3:21	+10	43.04	9.96	11.054	0.815	11.869	1	11.869	10.900	10.99	0.200	1755	19130	296	1478	144	0.55
6	3:28	+12	40.99	12.01	5.837	0.831	6.668	0.56	11.906	11.100	12.98	0.200	1750	19425	915	4575	474	
7	3:35	+14	39.06	13.94	5.779	0.846	6.625	0.56	11.831	11.300	14.94	0.200	1800	20340	360	1800	180	
8	3:44	+16	37.06	15.94	5.490	0.862	6.352	0.56	11.343	11.500	16.97	0.200	1800	20700	9	45	4	
9	3:59	+18	35.00	18.00	5.458	0.878	6.336	0.56	11.315	11.700	19.01	0.200	1770	20709	473	2365	235	
10	4:22	+20	32.99	20.01	9.716	0.894	10.610	1	10.610	11.900	20.74	0.200	1780	21182	4181	1721	1048	0.57
11	4:37	+21.5	31.54	21.46	4.898	0.910	5.808	0.56	10.372	12.100	22.73	2.229	no sample					
12	n/a	+25	29.00	24.00	15.76	0.926	15.762	1.1 *	14.329	14.329		14.33	1770	25363	25363			0.56

* consideration of flow loss between diversion valve and buffalo

Interval thickness	Relative flow/conductivity	Check	Relative mass flux	Check	c*Δz	Relative concentration	Check	Interval midpoint	Interval midpoint	Depth below ground	Depth below ground
(ft)	(unitless)		(unitless)		(pCi/ml * ft)	(unitless)		(ft)	(ft)	(ft)	(ft)
1.99	0.07	0.137	0.06	0.115	2945	0.79	1.578	1.00	1.00	49.51	49.51
2.02	3.53	7.121	3.48	7.021	3525	0.93	1.889	3.00	3.00	47.50	47.50
1.94	5.32	10.328	5.28	10.252	3409	0.94	1.826	4.98	4.98	45.52	45.52
2.10	0.16	0.335	0.25	0.534	5922	1.51	3.173	7.00	7.00	43.50	43.50
1.91	0.18	0.335	0.09	0.180	1819	0.51	0.975	9.01	9.01	41.50	41.50
2.05	0.16	0.335	0.14	0.280	3029	0.79	1.623	10.99	10.99	39.52	39.52
1.93	0.17	0.335	0.45	0.866	8830	2.45	4.731	12.98	12.98	37.53	37.53
2.00	0.17	0.335	0.17	0.341	3600	0.96	1.929	14.94	14.94	35.56	35.56
2.06	0.16	0.335	0.00	0.009	93	0.02	0.050	16.97	16.97	33.53	33.53
2.01	0.17	0.335	0.22	0.448	4754	1.27	2.547	19.01	19.01	31.50	31.50
1.45	0.23	0.335	0.99	3.956	6867	0.92	3.679	20.74	22.01	29.77	28.50
2.54	1.47	3.734						22.73		27.77	
24.00					1866						
		1.000000		1.000000			1.000000				

Table 6. Revised Data Analysis for HEX-18

Appendix A
General Engineering Laboratory (GEL) Mobile Lab Tritium Analysis Results

GEL ID	Client ID1	Client ID2	Date Sampled	Analyte	Method	Synonym	MDL	PQL	Units	Result	Uncertainty	Qualifier
55572001	01503-HEX-3-1		020402	Tritium	RADA-002	TRITIU	582	10942	PCL	654000	5180	
55572002	01503-HEX-3-2		020402	Tritium	RADA-002	TRITIU	663	12923	PCL	806000	6130	
55572003	01503-HEX-3-3		020402	Tritium	RADA-002	TRITIU	631	11691	PCL	687000	5530	
55572004	01503-HEX-3-4		020402	Tritium	RADA-002	TRITIU	626	11346	PCL	652000	5360	
55572005	01503-HEX-3-5		020402	Tritium	RADA-002	TRITIU	640	11460	PCL	648000	5410	
55572006	01503-HEX-3-6		020402	Tritium	RADA-002	TRITIU	638	11458	PCL	651000	5410	
55572007	01503-HEX-3-7		020402	Tritium	RADA-002	TRITIU	638	11298	PCL	633000	5330	
55572008	01503-HEX-3-10B		013102	Tritium	RADA-002	TRITIU	640	1330	PCL	-265	345	U

GEL ID	Client ID1	Client ID2	Date Sampled	Analyte	Method	Synonym	MDL	PQL	Units	Result	Uncertainty	Qualifier
55684001	01503-HEX-4-1		020602	Tritium	RADA-002	TRITIU	639	8639	PCL	364000	4000	
55684002	01503-HEX-4-2		020602	Tritium	RADA-002	TRITIU	687	10667	PCL	527000	4990	
55684003	01503-HEX-4-3		020602	Tritium	RADA-002	TRITIU	669	9969	PCL	469000	4650	
55684004	01503-HEX-4-4		020602	Tritium	RADA-002	TRITIU	666	10426	PCL	520000	4880	
55684005	01503-HEX-4-5		020602	Tritium	RADA-002	TRITIU	666	9806	PCL	456000	4570	
55684006	01503-HEX-4-6		020602	Tritium	RADA-002	TRITIU	663	9843	PCL	461000	4590	
55684007	01503-HEX-4-7		020602	Tritium	RADA-002	TRITIU	638	8838	PCL	381000	4100	
55684008	01503-HEX-4-8		020602	Tritium	RADA-002	TRITIU	644	8824	PCL	377000	4090	
55684009	01503-HEX-4-9		020602	Tritium	RADA-002	TRITIU	643	9023	PCL	396000	4190	
55684010	01503-HEX-4-2B		013102	Tritium	RADA-002	TRITIU	666	1408	PCL	-111	371	U

GEL ID	Client ID1	Client ID2	Date Sampled	Analyte	Method	Synonym	MDL	PQL	Units	Result	Uncertainty	Qualifier
55955001	01503-HEX18-1		021102	Tritium	RADA-002	TRITIU	593	18233	PCL	1780000	8820	
55955002	01503-HEX18-2		021102	Tritium	RADA-002	TRITIU	608	16928	PCL	1480000	8160	
55955003	01503-HEX18-3		021102	Tritium	RADA-002	TRITIU	623	18523	PCL	1740000	8950	
55955004	01503-HEX18-4		021102	Tritium	RADA-002	TRITIU	609	18369	PCL	1750000	8880	
55955005	01503-HEX18-4B		013102	Tritium	RADA-002	TRITIU	616	1278	PCL	-244	331	U
55955006	01503-HEX18-5		021102	Tritium	RADA-002	TRITIU	625	18665	PCL	1770000	9020	
55955007	01503-HEX18-6		021102	Tritium	RADA-002	TRITIU	630	18690	PCL	1750000	9030	
55955008	01503-HEX18-7		021102	Tritium	RADA-002	TRITIU	622	18602	PCL	1760000	8990	
55955009	01503-HEX18-8		021102	Tritium	RADA-002	TRITIU	616	18416	PCL	1750000	8900	
55955010	01503-HEX18-9		021102	Tritium	RADA-002	TRITIU	618	18878	PCL	1830000	9130	
55955011	01503-HEX18-10		021102	Tritium	RADA-002	TRITIU	597	18237	PCL	1770000	8820	
55955012	01503-HEX18-11		021102	Tritium	RADA-002	TRITIU	618	18558	PCL	1770000	8970	
55955013	01503-HEX18-12		021102	Tritium	RADA-002	TRITIU	625	18725	PCL	1780000	9050	
55955014	01503-HEX18-13		021102	Tritium	RADA-002	TRITIU	619	18579	PCL	1760000	8980	

Appendix B
Nearby Cone Penetrometer Testing (CPT) Results

Data for comparison of Cone Penetrometer Tests Upgradient of HEX Wells and EBF Testing at HEX wells; Prepared by Jeff Thibault

Jeff's CPT sample results		Location HCPT-03 is approximately 85 ft upgradient of HEX-3						SRS_E 56967.72 SRS_N 71315.0 Elev. 235.2				
GEL ID	**Client ID1**	**Client ID2**	**Date Sampled**	**Analyte**	**Method**	**Synonym**	**MDL**	**PQL**	**Units**	**Result**	**Uncertainty**	**Qualifier**
54993005	HCPT-03-26		012202	Tritium	RADA-002	TRITIU	627	14267	PCL	1010000	6820	
54993006	HCPT-03-31		012202	Tritium	RADA-002	TRITIU	632	26232	PCL	3560000	12800	
54993007	HCPT-03-36		012202	Tritium	RADA-002	TRITIU	631	24431	PCL	3070000	11900	
54993008	HCPT-03-41		012202	Tritium	RADA-002	TRITIU	554	23354	PCL	3200000	11400	
54993009	HCPT-03-50		012202	Tritium	RADA-002	TRITIU	635	9435	PCL	415000	4400	
	HCPT-03-##	## is sample depth below surface (ie, midpoint of 2-ft sample screen)										
	Yellow samples were collected stratigraphically from the elevation of the HEX-3 well screen											
Greg's EBF sample results												
GEL ID	**Client ID1**	**Client ID2**	**Date Sampled**	**Analyte**	**Method**	**Synonym**	**MDL**	**PQL**	**Units**	**Result**	**Uncertainty**	**Qualifier**
55572001	01503-HEX-3-1		020402	Tritium	RADA-002	TRITIU	582	10942	PCL	654000	5180	
55572002	01503-HEX-3-2		020402	Tritium	RADA-002	TRITIU	663	12923	PCL	806000	6130	
55572003	01503-HEX-3-3		020402	Tritium	RADA-002	TRITIU	631	11691	PCL	687000	5530	
55572004	01503-HEX-3-4		020402	Tritium	RADA-002	TRITIU	626	11346	PCL	652000	5360	
55572005	01503-HEX-3-5		020402	Tritium	RADA-002	TRITIU	640	11460	PCL	648000	5410	
55572006	01503-HEX-3-6		020402	Tritium	RADA-002	TRITIU	638	11458	PCL	651000	5410	
55572007	01503-HEX-3-7		020402	Tritium	RADA-002	TRITIU	638	11298	PCL	633000	5330	
55572008	01503-HEX-3-10B		013102	Tritium	RADA-002	TRITIU	640	1330	PCL	-265	345	U

Location_ID	Sample Depth_ID	SRS_E	SRS_N	UTM_E	UTM_N	Ground_ Elevation	Sample Top_Depth	Sample Base_Depth	Sample Top_Elevation	Sample Base_Elevation	pH	Tritium_Result	Tritium_Unit
HCPT01	30	57816.52	71434.88			244.11	29	31	215.11	213.11		2,270,000	PCL
HCPT01	35	57816.52	71434.88			244.11	34	36	210.11	208.11		1,880,000	PCL
HCPT01	40	57816.52	71434.88			244.11	39	41	205.11	203.11		729,000	PCL
HCPT01	45	57816.52	71434.88			244.11	44	46	200.11	198.11		331,000	PCL
HCPT01	52	57816.52	71434.88			244.11	51	53	193.11	191.11		1,160,000	PCL
HCPT01	65	57816.52	71434.88			244.11	64	66	180.11	178.11		173,000	PCL
HCPT01	74	57816.52	71434.88			244.11	73	75	171.11	169.11		74,700	PCL
HCPT01	90	57816.52	71434.88			244.11	89	91	155.11	153.11		178,000	PCL
HCPT01	119	57816.52	71434.88			244.11	118	120	126.11	124.11		70,200	PCL

highlighted samples correspond approximately to HEX-18 screen zone

Appendix B

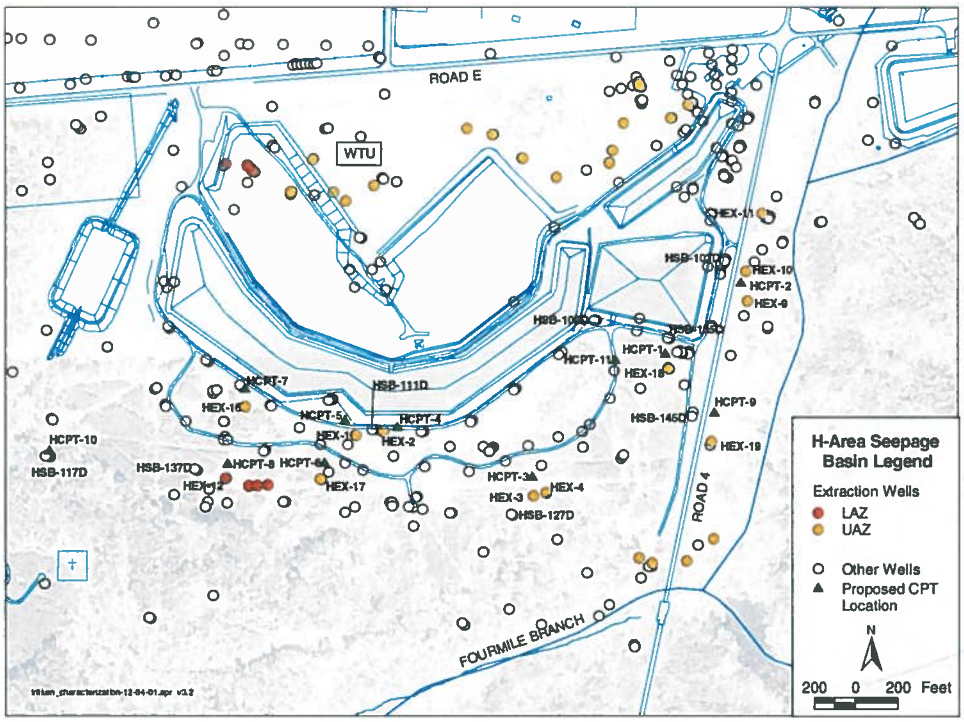
ROAD E
WTU
ROAD 4
FOURMILE BRANCH
HCPT-10
HSB-117D
HSB-137D
HCPT-8
HCPT-6
HEX-12
HEX-17
HCPT-7
HEX-16
HCPT-5
HEX-1
HCPT-4
HEX-2
HSB-111D
HCPT-3
HEX-3
HEX-4
HSB-127D
HCPT-11
HCPT-1
HEX-18
HSB-145D
HCPT-9
HEX-19
HEX-11
HEX-10
HCPT-2
HEX-9
H-Area Seepage Basin Legend
Extraction Wells
LAZ
UAZ
Other Wells
Proposed CPT Location
N
200 0 200 Feet